



# Preclinical Pharmacology of [2-(3-Fluoro-5-Methanesulfonylphenoxy)Ethyl](Propyl)amine (IRL790), a Novel Dopamine Transmission Modulator for the Treatment of Motor and Psychiatric Complications in Parkinson Disease<sup>[S]</sup>

 Susanna Waters, Clas Sonesson,  Peder Svensson, Joakim Tedroff, Manolo Carta, Elisabeth Ljung, Jenny Gunnergren, Malin Edling, Boel Svanberg, Anne Fagerberg, Johan Kullingsjö, Stephan Hjorth, and Nicholas Waters

*Integrative Research Laboratories Sweden AB, Göteborg, Sweden (S.W., C.S., P.S., J.T., E.L., J.G., M.E., B.S., A.F., J.K., N.W.); Pharmacilator AB, Valda, Sweden (S.H.); Department of Molecular and Clinical Medicine, Institute of Medicine, The Sahlgrenska Academy at Gothenburg University, Gothenburg, Sweden (S.H.); Department of Biomedical Sciences, University of Cagliari, Cagliari, Italy (M.C.); Department of Pharmacology, Gothenburg University, Gothenburg, Sweden (S.W.); and Department of Clin Neuroscience, Karolinska Institute, Stockholm, Sweden (J.T.)*

Received December 18, 2019; accepted April 2, 2020

## ABSTRACT

IRL790 [2-(3-fluoro-5-methanesulfonylphenoxy)ethyl](propyl)amine, mesdopetam) is a novel compound in development for the clinical management of motor and psychiatric disabilities in Parkinson disease. The discovery of IRL790 was made applying a systems pharmacology approach based on in vivo response profiling. The chemical design idea was to develop a new type of DA D3/D2 receptor type antagonist built on agonist rather than antagonist structural motifs. We hypothesized that such a dopamine antagonist with physicochemical properties similar to agonists would exert antidyskinetic and antipsychotic effects in states of dysregulated dopaminergic signaling while having little negative impact on physiologic dopamine transmission and, hence, minimal liability for side effects related to dopamine-dependent functions. At the level of in vivo pharmacology, IRL790 displays balancing effects on aberrant motor phenotypes, reducing L-DOPA-induced dyskinesias in the rodent 6-hydroxydopamine lesion model and reducing psychostimulant-induced locomotor hyperactivity elicited by pretreatment with either D-amphetamine or dizocilpine, without negatively impacting normal motor performance. Thus, IRL790 has the ability to normalize the behavioral phenotype in hyperdopaminergic as well as hypoglutamatergic states. Neurochemical and immediate

early gene (IEG) response profiles suggest modulation of DA neurotransmission, with some features, such as increased DA metabolites and extracellular DA, shared by atypical antipsychotics and others, such as increased frontal cortex IEGs, unique to IRL790. IRL790 also increases extracellular levels of acetylcholine in the prefrontal cortex and ventral hippocampus. At the receptor level, IRL790 appears to act as a preferential DA D3 receptor antagonist. Computational docking studies support preferential affinity at D3 receptors with an agonist-like binding mode.

## SIGNIFICANCE STATEMENT

This paper reports preclinical pharmacology along with molecular modeling results on IRL790, a novel compound in clinical development for the treatment of motor and psychiatric complications in advanced Parkinson disease. IRL790 is active in models of perturbed dopaminergic and glutamatergic signaling, including rodent 6-hydroxydopamine L-DOPA-induced dyskinesias and psychostimulant-induced hyperactivity, in a dose range that does not impair normal behavior. This effect profile is attributed to interactions at dopamine D2/D3 receptors, with a 6- to 8-fold preference for the D3 subtype.

## Introduction

The key pathophysiology of PD involves loss of dopaminergic and noradrenergic neurons in the substantia nigra and locus coeruleus, respectively, which is associated with severe

motor symptoms and progressive autonomic and neurocognitive dysfunctions (Kalia and Lang, 2015; Vermeiren and De Deyn, 2017). Other subcortical, cortical, and autonomic pathologies contribute to nonmotor symptoms in PD. It has been suggested that corticostriatal dysconnectivity and plasticity are key drivers for both core symptoms of PD and adverse effects emerging with long-term dopaminergic treatment (Villalba and Smith, 2018).

Involuntary movements occurring on L-DOPA treatment (LIDs) remain an unmet clinical need since the introduction of L-dopa in the 1970s. An estimated 40% of patients with PD develop LIDs within 4–6 years of L-DOPA treatment, and over time, it afflicts almost all patients (Ahlskog and Muentner,

This work was funded by Integrative Research Laboratories Sweden AB, Sweden.

Part of this work was presented as a poster presentation at the following workshop: Waters N, et al. (2016) Pharmacology of IRL790, a psychomotor stabilizer for the treatment of L-dopa induced dyskinesias and psychosis in Parkinson's disease. *Dopamine 2016 Conference*; 2016 Sept 5–9; Vienna, Austria. We-66C.

<https://doi.org/10.1124/jpet.119.264226>.

[S] This article has supplemental material available at [jpet.aspetjournals.org](http://jpet.aspetjournals.org).

2001). The pathogenetic mechanisms underlying the development of motor complications emerging with long-term L-DOPA treatment are not fully clarified. One major hypothesis is the impact of nonphysiologic fluctuations in striatal dopamine release, leading to maladaptive changes in dopaminergic and glutamatergic transmission pre- and postsynaptically (Cenci, 2014). Much focus has been on the impact of chronic L-DOPA treatment, but it has also been suggested that dopamine denervation per se is the central cause of LIDs (Borgkvist et al., 2018). Both D1 and D2/D3 receptor signaling have been implied in this context.

The development of LIDs is strongly associated with augmented DA D1 receptor-mediated neurotransmission in medium spiny neurons of the direct striatonigral pathway (Feyder et al., 2011). Upregulation of DA D3 receptors has been pointed out as a key factor contributing to dysregulated D1 receptor-mediated signaling through D1–D3 receptor-receptor interactions, including heteromerization interfering with D1 receptor internalization and intracellular signaling (Marcellino et al., 2008).

Striatal dopamine D3 receptors are upregulated in 6-OHDA-lesioned rats treated with L-DOPA (Bordet et al., 1997) and in (1-methyl-4-phenyl-1,2,3,6-tetrahydropyridine)-treated primates (Bezard et al., 2003). Furthermore, increased DA D3 receptor binding in patients with PD and LIDs has been demonstrated using positron emission tomography (Payer et al., 2016). D3 receptor knockout reduces LIDs in mice (Solís et al., 2017), whereas L-DOPA treatment is reported to induce involuntary movements in nonparkinsonian rodents overexpressing D3 receptors (Cote et al., 2014).

In clinical practice, the main strategy to reduce L-DOPA-induced motor complications in PD is to reduce and adjust dopaminergic treatment to minimize fluctuations in plasma concentrations of the dopamine agonist used (Rascol et al., 2015). This can improve motor fluctuations but does not specifically address dyskinesias. Amantadine was recently introduced in an extended release formulation for treatment of LIDs (Sharma et al., 2018). Among the side effects, psychotic symptoms are likely related to the NMDA antagonist properties of amantadine, and psychotic symptoms are frequently observed in clinical studies on NMDA antagonists (Muir and Lees, 1995). An increased incidence of visual hallucinations was reported in a meta-analysis assessing Metabotropic glutamate receptor 5 antagonists in LIDs (Wang et al., 2018b). There are no other pharmacological treatments approved for LIDs. Surgical procedures, including deep brain stimulation, are used in some cases to alleviate dyskinesias and improve overall motor function in PD (Krack et al., 2017).

IRL790 (Sonesson et al., 2012) is a novel compound in development for the treatment of mental and motor complications in PD. The discovery of IRL790 was made applying an *in vivo* systems pharmacology approach (Waters et al., 2017). The strategy was to find compounds that could normalize

aberrant phenotypes linked to corticostriatal dysconnectivity through interactions with DA D2/D3 receptors. The original chemical design idea was to develop a new type of DA D2/D3 antagonist built on agonist rather than antagonist structural motifs. This would lead to compounds that mimic the specific receptor interactions of DA better, however, without displaying any intrinsic activity. A new series of compounds were discovered, among which IRL790 was selected for further development.

Preclinical assessment of IRL790 indicated a pharmacokinetic profile enabling oral administration and no safety concerns, which was corroborated in a phase 1a trial (IRLAB data on file). IRL790 is currently in clinical development, focusing on LIDs and PD psychosis. Results from a phase 1b study in PD were recently published, confirming a favorable safety profile and suggesting improvement of LIDs (Svenningsson et al., 2018).

This paper describes the preclinical pharmacology of IRL790 as investigated in normal and perturbed states, including rodent LIDs. The findings are discussed in terms of tentative receptor level mode of action based on *in vitro* assays, along with molecular modeling of G protein-coupled receptor-ligand interactions, which is focused on the dopamine D3 receptor.

## Materials and Methods

### Animals and Drugs

Male Sprague-Dawley rats were purchased from B&K Scanbur (Sollentuna, Sweden; locomotor recordings and tissue analysis in normal, non-pretreated rats), Charles River (Köln, Germany; microdialysis and MK-801 interaction study) or Taconic (Ejby, Denmark; AIMs study and D-amphetamine interaction). Rats weighed 160–180 g at the time of arrival and 220–260 g at the time of the *in vivo* pharmacology studies. Animals were housed five per cage with lights on between 06:00 and 18:00 at 22°C with free access to food and water. All experiments were carried out in accordance with Swedish animal protection legislation and with the approval of the local animal ethics committee in Gothenburg [Ethics application 1/2011 (AIMs study), 325/08 (locomotor recordings and tissue analysis), 287/10 (microdialysis)].

Locomotor recordings and *ex vivo* neurochemistry analysis were performed essentially as described in Waters et al. (2014). IRL790, synthesized in-house as HCl salt, was dissolved in physiologic saline (0.9% w/v NaCl) and injected subcutaneously in a volume of 5 ml/kg 4 minutes before start of locomotor activity recordings. For interaction studies, rats were pretreated with MK-801 (0.7 mg/kg; Sigma-Aldrich) or D-amphetamine (1.5 mg/kg; AKL, Sweden) injected intraperitoneally 90 or 10 minutes, respectively, before start of locomotor recordings.

For the gene map, the following drugs, all purchased from commercial suppliers, were administered: amantadine HCl (45–405 mg/kg), apomorphine HCl (0.12–1.1 mg/kg), aripiprazole (0.25–2.25  $\mu$ mol/kg), cariprazine HCl (1–3 mg/kg), clozapine (3–30 mg/kg), dihydroxidine HCl (3–10 mg/kg), donepezil (0.37–3.3 mg/kg), memantine HCl (3.3–10 mg/kg), quetiapine fumarate (11–100 mg/kg), risperidone (0.1–1 mg/kg), ropinirole HCl (1.1–10 mg/kg), and SCH23390 HCl (0.12–1.1 mg/kg). All drugs were

**ABBREVIATIONS:** ACh, acetylcholine; AIM, abnormal involuntary movement; AP, Anteroposterior; Arc, activity-regulated cytoskeleton-associated protein; CNS, central nervous system; DA, dopamine; DOPAC, 3,4-dihydroxyphenylalanine acid; DV, Dorsoventral; ECL2, second extracellular loop; Egr, early growth response protein; HEK-293, human embryonic kidney 293; 5-HIAA, 5-hydroxyindoleacetic acid; HPLC/EC, high-performance liquid chromatography/electrical detection; HPRT, hypoxanthine phosphoribosyltransferase; 5-HT, 5-hydroxytryptamine; HVA, homovanillic acid; IEG, immediate early gene; IRL790, ([2-(3-fluoro-5-methanesulfonylphenoxy)ethyl](propyl)amine), mesdopetam; LID, L-DOPA-induced dyskinesia; MFB, medial forebrain bundle; ML, Medialateral; 3-MT, 3-methoxytyramine; NA, noradrenaline; NM, normetanephrine; NMDA, N-methyl-D-aspartate; NPAS, neuronal PAS domain protein; Nptx2, pentraxin 2 6-OHDA 6-hydroxydopamine; PCR, polymerase chain reaction; PD, Parkinson disease; PDB, The Protein Data Bank; pfc, prefrontal cortex; PLS, partial least squares; RT, reverse transcription; TM, transmembrane helix w.c.

given subcutaneously in a volume of 5 ml/kg. Sixty-minute locomotor recordings followed by collection of brain tissue samples were performed as described below (sections *Locomotor Recordings* and *Ex Vivo Neurochemistry*).

### Locomotor Recordings

Locomotor activity was recorded for 60 minutes in sound and light-attenuating motility meter boxes (55 × 55 cm) with a maneuvering space of 41 × 41 cm [Digiscan activity monitor RZYCCM (16) TAO; Omnitech Electronics], generating a time series of *x*, *y* (horizontal activity), and *z* (vertical activity) position coordinates sampled at 25 Hz. Distance traveled was calculated based on horizontal coordinates and pooled into 5-minute periods. Results are presented as means, with error bars representing S.E.M. Repeated measures ANOVA with time as the repeated factor and treatment as a categorical between-group factor was performed, applying Mauchly's sphericity test and Greenhouse-Geisser and Huynh-Feldt adjusted significance tests, followed by post hoc Dunnett's test comparing IRL790 at different doses versus controls. TIBCO Statistica 13.5.0. was used for the statistical analyses.

### Ex Vivo Neurochemistry

Ex vivo neurochemical analysis was performed as described in Waters et al. (2017). Immediately after the behavioral activity recording sessions, animals were decapitated, and brains were dissected into striatum, cortex, and limbic region (containing the nucleus accumbens—both core and shell, most parts of the olfactory tubercle, and ventral pallidum). Tissue samples were immediately frozen and stored at −80°C until they were homogenized with perchloric acid (0.1 M), EDTA (5.37 mM), glutathione (0.65 mM), and  $\alpha$ -methyl-dopamine (0.25  $\mu$ M) as internal standard. Tissue eluates were analyzed with respect to tissue concentrations (nanogram per gram tissue) of the monoamine transmitters NA, DA, 5-HT, and corresponding amine and acid metabolites [NM, 3-metoxityramine (3-MT), DOPAC, HVA, and 5-hydroxyindoleacetic acid (5-HIAA)] by HPLC/EC. The HPLC/EC method is based on two chromatographic separations dedicated for amines or acids. Two chromatographic systems share a common autoinjector with a 10-port valve and two sample loops for simultaneous injection on the two systems. Both systems are equipped with a reverse phase column [Luna C18(2), particle size 3  $\mu$ m, 50 × 2 mm i.d.; Phenomenex], and electrochemical detection is accomplished at two potentials on glassy carbon electrodes (MF-1000; Bioanalytical Systems, Inc.). Neurochemical results are presented as percent of control group means. Error bars = S.E.M. Statistics: Student's *t* test (two-tailed) versus controls. \**P* < 0.05, \*\**P* < 0.01, \*\*\**P* < 0.001.

### Microdialysis

In vivo brain microdialysis experiments were performed as described in Waters et al. (1993) and Ponten et al. (2010), with some minor modifications. Microdialysis probes were implanted by stereotaxic surgery 40–48 hours before the experiments during isoflurane inhalation anesthesia. Coordinates were calculated relative to bregma (dorsal striatum: AP +1.0, ML  $\pm$ 2.6, DV −6.2; prefrontal cortex: AP +3.2, ML  $\pm$ 1.2, DV −4.0) according to Paxinos and Watson (1986). After surgery, the rats were housed individually in regular cages and were allowed free movement throughout the experiment. The perfusion medium for dialysis was a Ringer's solution containing, in micromolars: NaCl, 140; CaCl<sub>2</sub>, 1.2; KCl, 3.0; MgCl<sub>2</sub>, 1.0; and ascorbic acid, 0.04. The rats were perfused for around 60 minutes before baseline sampling began to obtain a balanced fluid exchange. Samples were drawn every 20 minutes. To establish a baseline, five fractions of dialysate were collected, and the last three were used to calculate baseline levels of each analyte. After establishment of baseline, IRL790 was administrated subcutaneously in a volume of 5 ml/kg, with 0.9% NaCl (saline) as vehicle. Vehicle controls, run in a separate

experiment, received saline. The monoamine transmitters (NA, DA, 5-HT) as well as their amine (NM, 3-MT) and acid (DOPAC, 5-HIAA, HVA) metabolites were followed for 180 minutes and quantified by HPLC/EC. After the experiment, the rats were uncoupled from the perfusion pump and decapitated. Their brains were rapidly taken out and kept in Accustain 1 or 2 days before carefully slicing the brain to verify correct probe position. Only results from rats with correctly positioned dialysis probes were included in the subsequent analysis. Microdialysis data are expressed as means  $\pm$  S.E.M. in percentage of baseline levels. Baseline was defined as the mean level of the three fractions collected immediately before administration of test compound.

In a separate in vivo microdialysis experiment, levels of ACh were assessed in extracellular fluid collected from the prefrontal cortex and ventral hippocampus (coordinates: AP −5.2, ML 4.8, DV −7.5 (Paxinos and Watson 1986) by means of liquid chromatography/tandem mass spectrometry, as described previously (Jerlhag et al., 2012).

Dialysis data were analyzed by a two-way ANOVA with treatment as independent variable and time as repeated measure. If significant, the two-way ANOVA was followed by a Fisher's least significant difference test. Significance between vehicle and IRL790 treatment at specific time points is indicated in the graphs as follows: \**P* < 0.05, \*\**P* < 0.01, \*\*\**P* < 0.001.

### AIMs

IRL790 was tested in two independent studies, in-house and by an external laboratory, in the 6-OHDA model of AIMs (Lundblad et al., 2005). In this model, the repeated administration of L-DOPA to rats subjected to unilateral 6-OHDA lesions of the nigrostriatal dopaminergic system elicits adverse involuntary movements, affecting the orofacial region, the limbs, and the trunk. The sum of AIMs scored in orofacial region, limbs, and trunk is denoted total AIMs or, alternatively, composite AIMs score. Both studies were performed using rats subjected to unilateral injections of 6-OHDA (Sigma-Aldrich) into the nigrostriatal fiber bundle, as described previously (Lundblad et al., 2005). In the in-house study, 48 male Sprague-Dawley rats were stereotactically injected with 6-OHDA (10  $\mu$ g in 2  $\mu$ l saline with 0.1% ascorbic acid) into the MFB to achieve complete unilateral dopaminergic denervation. Half of the rats were injected in the right side, and the other half were injected in the left side of MFB. Three weeks after lesion, animals were subjected to an apomorphine-induced rotation test (0.1 mg/kg, i.p.) to verify the success of the lesion procedure. Animals were then given daily injection of L-DOPA at 6.5 mg/kg dose s.c. (plus benserazide 12 mg/kg) for about 3 weeks to establish full expression of dyskinesias. Twelve rats showing significant dyskinesias were allocated to two different groups (*n* = 6/group) that were balanced to have similar baseline dyskinesia scores; one group served as a control group, receiving L-DOPA only, and the other group received L-DOPA + IRL790, 33  $\mu$ mol/kg s.c. (i.e., 10 mg/kg), on a separate day of drug test following baseline scoring. Dyskinesias were scored every 20 minutes (1 minute per rat) for the entire time course of L-DOPA (about 2 hours). Scoring was performed manually by two persons blinded to treatment, and the mean values were used for subsequent statistical calculations and graphs. Limb, axial, and orolingual dyskinesias were evaluated individually and summed into composite scores.

In the external study, 80 female Sprague-Dawley rats were stereotactically injected with 6-OHDA (14  $\mu$ g in 4  $\mu$ l) into the right MFB to achieve complete unilateral dopaminergic denervation. Three weeks after lesion, animals were subjected to the amphetamine-induced rotation test (2.5 mg/kg, i.p.) to verify the success of the lesion procedure. Only animals rotating at least six turns per minute (over a 90-minute period) were used in the study. Animals were then given daily injections of L-DOPA at 6 mg/kg dose s.c. (plus benserazide 10 mg/kg) for about 4 weeks to establish full expression of dyskinesias. In total, 32 rats showing significant and stable dyskinesias were

allocated to four different groups ( $n = 8/\text{group}$ ), which were balanced to have similar baseline dyskinesia scores; one group served as control (L-DOPA only), and the other groups received L-DOPA + IRL790 at three different doses. Dyskinesias were scored every 20 minutes for the entire time course of L-DOPA (about 2 hours). Limb, axial, and orolingual dyskinesias were evaluated individually, and the composite score was then calculated. IRL790 was initially tested at 1, 3, and 10 mg/kg s.c., given 20 minutes before L-DOPA ( $n = 8 \text{ rats/group}$ ). Subsequently, the effects of 20 mg/kg s.c. were tested in a separate experimental session ( $n = 7 \text{ rats/group}$ ; controls received L-DOPA only).

Graphs display means of composite dyskinesia scores, with error bars representing S.E.M. Graphs with medians and quartiles are provided as Supplementary Data. In the external study, a repeated measures ANOVA was performed on the composite scores, applying Mauchly's sphericity test and Greenhouse-Geisser and Huynh-Feldt adjusted significance tests, followed by post hoc Dunnett's test comparing IRL790 at different doses versus controls. The results from the test of 20 mg/kg + L-DOPA versus L-DOPA-treated controls were analyzed separately. The results were confirmed with nonparametric tests: Kruskal-Wallis test for the initial dose-response study and Mann-Whitney  $U$  test comparing 20 mg/kg versus L-DOPA controls, based on total composite scores. An integrated dose-response analysis using total composite scores collected from both experimental sessions was undertaken, fitting a sigmoid curve to the data using the TIBCO Spotfire software. In the in-house study, statistical comparison between control and IRL790 treatment was performed using ANOVA with time as repeated measure, which was confirmed with Mann-Whitney  $U$  test and based on total composite scores.

## Analysis of mRNA

For ex vivo mRNA analysis, brains were removed immediately after the completion of locomotor recordings and were dissected into four regions: limbic system (containing nucleus accumbens, most parts of the olfactory tubercle, ventral pallidum, and amygdala), striatum, frontal cortex, and hippocampus. Tissue samples were stored at  $-80^\circ\text{C}$  until further processing. Total RNA was prepared using the guanidine isothiocyanate method (Chomczynski and Sacchi, 1987). RNA pellets were dissolved in RNase-free water and stored at  $-80^\circ\text{C}$ . The RNA concentration was determined spectrophotometrically using a NanoDrop ND-1000 (Saveen Werner, Limhamn, Sweden), and the quality and integrity of random samples were checked using an Experion automated electrophoresis system (Bio-Rad, Sundbyberg, Sweden). Reverse transcription was performing using a SuperScript III kit (Invitrogen, Groningen, Netherlands) as follows: 1  $\mu\text{g}$  of total RNA was mixed with 5  $\mu\text{l}$   $2\times$  RT Reaction Mix and 1  $\mu\text{l}$  of RT Enzyme Mix. The reaction volume was adjusted to 10  $\mu\text{l}$  with RNase-free water. The mixture was incubated at  $25^\circ\text{C}$  for 10 minutes,  $50^\circ\text{C}$  for 30 minutes, and then  $85^\circ\text{C}$  for 5 minutes. *Escherichia coli* RNase H (1 U) was added, and the reaction mixture was incubated at  $37^\circ\text{C}$  for 20 minutes and then  $85^\circ\text{C}$  for 5 minutes. The final cDNA was diluted 40 times in 10 mM Tris-HCl and 0.1 mM EDTA (pH 7.8) and stored at  $-20^\circ\text{C}$ .

**Single-Plex Real-Time PCR.** For all genes, 0.7  $\mu\text{l}$  of cDNA solution was incorporated in a reaction mixture containing  $1\times$  PCR buffer, 0.2 mM deoxynucleotide triphosphate, 3.7 mM magnesium chloride, 0.15 mM SYBR green, 0.4  $\mu\text{M}$  of each primer, and 1 U of Taq polymerase (Invitrogen, Stockholm, Sweden) in a final volume of 25  $\mu\text{l}$ . Real-time PCR was performed using a CFX96 Real-Time PCR Detector (Bio-Rad) with the following cycling conditions: initial denaturation at  $95^\circ\text{C}$  for 1 minute followed by 40 cycles of  $95^\circ\text{C}$  for 10 seconds,  $56^\circ\text{C}$  for 10 seconds, and  $72^\circ\text{C}$  for 10 seconds. Primer sequences were as follows: HPRT (accession number NM 012583), sense 5'-GGC CAG ACT TGT TGG ATT TG-3', antisense 5'-CCG CTG TCT TTT AGG CTT TG-3'; cyclophilin A (accession number M19533), sense 5'-GTC TCT TTT CGC CGC TTG CT-3', antisense 5'-TCT GCT GTC TTT GGA ACT TTG TCT G-3'; Arc (accession number U19866),

sense 5'-GTC CCA GAT CCA GAA CCA CA-3', antisense 5'-CCT CCT CAG CGT CCA CAT AC-3'; and *cfos* (proto-oncogene accession number NM 022197), sense 5'-CAG AGC ATC GGC AGA AGG-3', antisense 5'-AGT TGA TCT GTC TCC GCT TGG-3. The sample DNA concentration was estimated using a standard curve constructed for each gene using serial dilutions of purified PCR products. Correct PCR products were identified by agarose gel electrophoresis, purified using the PCR Purification Kit (Qiagen, Sollentuna, Sweden), sequenced at MWG-Biotech AG (Ebersberg, Germany), and analyzed routinely by melting-curve analysis to confirm the specificity of the reaction. Yields of Arc and *cfos* genes were normalized using the geometric mean of the yields of HPRT and cyclophilin A.

**TaqMan Single and Duplex PCR.** The real-time PCR reaction consisted of 10  $\mu\text{l}$  Sso Advanced Universal Probes Supermix, 1  $\mu\text{l}$  primer/probe, 1  $\mu\text{l}$  reference gene or 1  $\mu\text{l}$  MQ water, and 8  $\mu\text{l}$  of cDNA (diluted 40 times from RT-PCR). Real-time PCR reactions were performed in a CFX96 Real-Time PCR Detector (Bio-Rad) with the following cycling conditions: initial denaturation at  $95^\circ\text{C}$  for 2 minutes followed by 40 cycles of  $95^\circ\text{C}$  for 5 seconds and  $60^\circ\text{C}$  for 30 seconds. All genes of interest were labeled with the fluorophore carboxyfluorescein on the 5' end, and reference genes were labeled with Hexachloro-fluorescein. TaqMan primers and probes were synthesized by Bio-Rad (Coralville, IA) and used according to the manufacturing protocol. The gene *homer1a* (in-house designed, glycine-leucine-glycine-phenylalanine-domain protein accession number U92079.1) sense 5'-TGGCAT AATACCTTACCTTGAGT-3', antisense 5'-GCACTCTACAG TATA-TACGAGCC-3', probe sequence: TTGGTTTCTAAAACTCTACT GCT (Bio-Rad), was analyzed in duplex with the reference gene *Ppia* (cyclophilin A, peptidyl-propyl cis-trans isomerase qRnoCIP0050815). Early growth response protein 1 (*Egr1*, Bio-Rad Assay ID qRno-CEP0022872, chromosome location 18:27371314-27371422) was analyzed in duplex with the reference gene HPRT (qRnoCEP0050840). Neuronal Nptx2 (pentraxin 2 qRnoCEP0030302) and neuronal PAS domain protein 4 (*Npas4*; qRnoCEP0029461) were both analyzed in singleplex. *Ppia* (cyclophilin A) and HPRT were used for normalization.

Results are presented as means  $\pm$  S.E.M, expressed as percentages of control group means. Statistical significance was assessed using Student's  $t$  test (two-tailed) versus controls:  $*P < 0.05$ ,  $**P < 0.01$ ,  $***P < 0.001$ .

For the gene mapping on multiple compounds, multivariate analysis was performed as described in Waters et al. (2017), applying PLS regression analysis using a discriminant variable block denoting doses of test compounds as dependent (Y) variable block ( $n$  Y variables), and mRNA levels in each brain region analyzed, as independent variable block ( $4 \times 6 = 24 \times$  variables). The independent variables were subject to zero mean and unit variance scaling and block scaled by IEG. Statistical significance was determined by cross validation. Multivariate analyses were carried out using SIMCA 16.0 (Umetrics, Inc.). Results are visualized as  $w^*c$  loading plots showing clusters and effect patterns among the test compounds analyzed.

## In Vitro Pharmacology

All in vitro pharmacology studies were carried out using standard assays by the laboratories of Cerep, France, (see <https://www.eurofinsdiscoveryservices.com/cms/cms-content/services/in-vitro-assays/>). A broad binding screen (ExpresSProfile Panel, 55 targets, list provided as Supplemental Data) covering receptors, enzymes, and transporters related to all major CNS neurotransmitters was performed at 10  $\mu\text{M}$  IRL790, run in triplicate at each binding target, followed by determination of  $K_i/\text{IC}_{50}$  at selected targets displaying at least  $\sim 20\%$  inhibition of control specific binding. The specific ligand binding to the receptors is defined as the difference between the total binding and the nonspecific binding determined in the presence of an excess of unlabeled ligand. Inhibition of control specific binding was calculated as  $(100 - [(\text{measured specific binding}/\text{control specific binding}) \times 100])$  obtained in the presence of the test compound (IRL790). For  $\text{IC}_{50}/K_i$  determination, IRL790 was tested at eight concentrations in duplicates.

TABLE 1  
IRL790 IC<sub>50</sub>/K<sub>i</sub> values for selected targets

Assay	Radioligand (Type)	Source	IC <sub>50</sub> (μM)	K <sub>i</sub> (μM)	Reference Compound
D3 (h)	[ <sup>3</sup> H]Me-spiperone (antagonist)	CHO	0.41	0.09	(+)-butaclamol
D2S (h)	[ <sup>3</sup> H]Me-spiperone (antagonist)	HEK-293	1.6	0.54	(+)-butaclamol
D2S (h)	[ <sup>3</sup> H]7-OH-DPAT (agonist)	HEK-293	1.9	0.75	7-OH-DPAT
σ1 (h)	[ <sup>3</sup> H](+)-pentazocine (agonist)	Jurkat	1.7	0.87	Haloperidol
5-HT1A (h)	[ <sup>3</sup> H]8-OH-DPAT (agonist)	HEK-293	3.6	2.2	8-OH-DPAT
5-HT2A (h)	[ <sup>125</sup> I](±)DOI (agonist)	HEK-293	9.9	7.4	(±) DOI
Norepinephrine transporter (h)	[ <sup>3</sup> H]nisoxetine (inhibitor)	CHO	11	8	Protriptyline
5-HT7 (h)	[ <sup>3</sup> H]LSD (agonist)	CHO	29	11	Serotonin
α2C (h)	[ <sup>3</sup> H]RX 821002 (antagonist)	CHO	45	15	Yohimbine
α1 (nonselective; rat)	[ <sup>3</sup> H]prazosin (antagonist)	Rat cerebral cortex	>100	—	Prazosin
α2A (h)	[ <sup>3</sup> H]RX 821002 (antagonist)	CHO	>100	—	Yohimbine
Dopamine transporter (h)	[ <sup>3</sup> H]BTCP (antagonist)	CHO	>100	—	BTCP
H3 (h)	[ <sup>3</sup> H]N-α-Me-histamine (agonist)	CHO	>100	—	R(α)-Me- histamine
MAO-A (rat)	[ <sup>3</sup> H]Ro 41-1049 (inhibitor)	Rat cerebral cortex	>100	—	Clorgyline
MAO-B (rat)	[ <sup>3</sup> H]Ro 19-6327 (inhibitor)	Rat cerebral cortex	>100	—	(R)-deprenyl

The abbreviation (h) denotes human recombinant protein. MAO, Monoamine oxidase; BTCP, N-[1-(2-benzo(b)thiophenyl)cyclohexyl]piperidine; 7-OH-DPAT, 7-hydroxy-2-(di-N-propylamino)tetralin; 8-OH-DPAT, 8-hydroxy-2-(di-N-propylamino)tetralin; DOI, 1-(2,5-dimethoxy-4-iodophenyl)-2-aminopropane; LSD, Lysergic acid diethyl amide

IC<sub>50</sub> values (concentration causing a half-maximal inhibition of control specific binding) were determined by nonlinear regression analysis of the competition curves generated with mean replicate values using Hill equation curve fitting. The inhibition constants (K<sub>i</sub>) were calculated using the Cheng-Prusoff equation ( $K_i = IC_{50}/[1 + (L/K_D)]$ , where L = concentration of the radioligand in the assay, and K<sub>D</sub> = affinity of the radioligand for the receptor). Source of cells were either CHO or human embryonic kidney 293 (HEK-293). Details of specific binding assays are given in Table 1.

For selected receptor targets, additional in vitro studies were performed, assessing intrinsic activity and antagonist properties. Assay details are provided in Table 2.

EC<sub>50</sub> values (concentration producing a half-maximal response) and IC<sub>50</sub> values (concentration causing a half-maximal inhibition of the control agonist response) were determined by nonlinear regression analysis of the concentration-response curves, generated with mean replicate values using Hill equation curve fitting:  $Y = D + [A - D]/[1 + (C/C_{50})^{n_H}]$ , where Y = response, A = left asymptote of the curve, D = right asymptote of the curve, C = compound concentration, C<sub>50</sub> = EC<sub>50</sub> or IC<sub>50</sub>, and n<sub>H</sub> = slope factor. This analysis was performed using software developed at Cerep (Hill software) and validated by comparison with data generated by the commercial software SigmaPlot 4.0 for Windows (1997 by SPSS Inc.). For the antagonists, the apparent dissociation constants (K<sub>B</sub>) were calculated using the modified Cheng-Prusoff equation  $K_B = IC_{50} / [1 + (A/EC_{50}A)]$ , where A = concentration of reference agonist in the assay, and EC<sub>50</sub>A = EC<sub>50</sub> value of the reference agonist.

## Computational Methods

The development of a structure model of the D2 receptor and the docking of IRL790 into the ligand binding site of dopamine D3 and D2

receptor structures were performed using the Molecular Operating Environment software (version 2019.01; Chemical Computing Group Inc., Montreal, QC, Canada). The X-ray crystal structure of the human dopamine D3 receptor (PDB entry 3PBL) was used for docking of IRL790 and as template for the development of a homology model of the human dopamine D2 receptor structure (Chien et al., 2010). The recently published dopamine D2 receptor structure complex with the antagonist risperidone PDB entry 6CM4 (Wang et al., 2018a) was evaluated and discarded as a structure model because of the atypical conformation of the receptor induced by risperidone. The C-terminal part of the second extracellular loop (ECL2) that constitutes the upper part (or the lid) of the orthosteric binding site adopts a unique open conformation in the D2R structure that is not present in the other 39 solved X-ray structures of monoaminergic G protein-coupled receptors with a resolution ≤ 3.0 Å.

## Results

### In Vivo Pharmacology

The pharmacological properties of IRL790 were investigated in a series of in vivo studies in rats, including models of psychosis and AIMs, based on disrupted dopaminergic or glutamatergic neurotransmission. Neurochemical biomarkers collected include monoaminergic indices assessed in brain tissue ex vivo and by in vivo brain microdialysis, as well as IEGs.

**Effects on Behavior.** In normal, non-pretreated rats, there was no significant effect on locomotor activity at 3.7–100 μmol/kg [significant effect of time,  $F(11,165) = 61.1$ ,

TABLE 2  
Agonist effects in cellular functional assays (human receptors)

Assay	EC <sub>50</sub>	Source	Measured Component	Reference
D2S	n.c. <sup>a</sup>	HEK-293 cells	Impedance	SOP 1C531
D3	n.c.	CHO cells	cAMP	SOP 1C374
5-HT1A	>1.0 × 10 <sup>-4</sup> M	HEK-293 cells	Impedance	SOP 1C913
5-HT2A	n.c.	HEK-293 cells	IP1	SOP 1C865

n.c., not calculable; SOP, standard operating procedures used by CEREP.

<sup>a</sup>EC<sub>50</sub> not calculable due to lack of effect. IP1, inositol monophosphate.



adjusted  $P < 0.00001$ , but not of treatment or time  $\times$  treatment; Fig. 1]. IRL790 was further investigated in two pharmacological rat models of psychosis, i.e., in rats displaying aberrant, hyperactive motor behavior due to pretreatment with the catecholamine releaser D-amphetamine (hyperdopaminergic state) or the glutamatergic NMDA receptor antagonist (+)-MK-801 (hypoglutamatergic state). IRL790 dose-dependently inhibited the behavioral activation following pretreatment with D-amphetamine or MK-801 (Figs. 2 and 3). In D-amphetamine-pretreated rats, there was a significant effect of treatment [ $F(4,15) = 18.918$ ,  $P = 0.00001$ ], time [ $F(11,165) = 36.23$ ,  $P < 0.00001$ ], and time  $\times$  treatment [ $F(44,165) = 2.35$ ,  $P = 0.00005$ , adjusted  $P < 0.05$ ]. Post hoc analysis indicated significant inhibition of locomotion at 33  $\mu\text{mol/kg}$  s.c. ( $P < 0.001$ ) and 100  $\mu\text{mol/kg}$  s.c. ( $P < 0.001$ ). Similar effects were observed in rats pretreated with MK-801; with a significant effect of treatment [ $F(4,15) = 10.1$ ,  $P = 0.00035$ ], time [ $F(11,165) = 53.9$ ,  $P < 0.000001$ ], and time  $\times$  treatment [ $F(44,165) = 3.09$ ,  $P < 0.000001$ , adjusted  $P < 0.05$ ]. Post hoc analysis indicated significant reductions at 33  $\mu\text{mol/kg}$  s.c. ( $P < 0.05$ ) and 100  $\mu\text{mol/kg}$  s.c. ( $P < 0.01$ ). These pharmacological effects were also present upon oral administration of similar doses of IRL790 (data not shown).

The potential antidyskinetic effects of IRL790 were investigated in rats subjected to unilateral 6-OHDA lesions of the nigrostriatal dopaminergic system, combined with repeated treatment with L-DOPA, which elicits adverse involuntary movements affecting the orofacial region, the limbs, and the trunk. Rat AIMs present many functional and phenomenological analogies to L-DOPA-induced dyskinesia in patients with PD (Cenci and Lundblad, 2005). IRL790 was tested in the 6-OHDA model in two independent studies, one run in-house and one run by an external laboratory (University of Cagliari).

Tested at IRLs laboratories, IRL790 at 33  $\mu\text{mol/kg}$  s.c. resulted in a near-complete suppression of total AIMs, which persisted during the full 2-hour experiment period (Fig. 4). Repeated measures ANOVA indicated a significant effect of time [ $F(6,60) = 28,729$ ,  $P < 0.000001$ ], treatment [ $F(1,10) = 125,21$ ,  $P < 0.000001$ ], and treatment  $\times$  time [ $F(6,60) = 17,416$ ,  $P < 0.000001$ ]. Nonparametric analysis confirmed statistical significance ( $P = 0.005$  vs. controls based on total composite scores). The total composite score was  $8.7 \pm 3.3$  points in the IRL790 + L-DOPA group, and  $56.8 \pm 2.8$  in controls receiving L-DOPA only. (Baseline total composite scores were  $47.9 \pm 5.1$  and  $48.1 \pm 5.5$  in the IRL790 and control groups, respectively.) Limb, orolingual, and axial AIMs were all equally reduced by IRL790 (data not shown).

In the external study, IRL790 was initially tested at 1, 3, and 10 mg/kg s.c., corresponding to 3.2, 9.6, and 32  $\mu\text{mol/kg}$  s.c., administered 20 minutes before L-DOPA ( $n = 8$  rats/group). As IRL790 did not appear to reduce the L-DOPA-induced motor activation in the test cages, a fourth dose of 20 mg/kg (64  $\mu\text{mol/kg}$ ) was tested in a separate session ( $n = 7$  rats/group). A dose-dependent antidyskinetic effect was observed with a reduction by approximately 40% in the total composite AIMs score as compared with the control group at 10 mg/kg and a 45% reduction at 20 mg/kg (Fig. 5). The repeated measures models indicated a significant effect of time [ $F(6,168) = 93.3$ ,  $P < 0.000001$ ] and treatment [ $F(3,28) = 6.2$ ,  $P = 0.002$ ] in the dose-response experiment as well as in the experiment testing only 20 mg/kg versus L-DOPA [time  $F(6,72) = 43$ ,

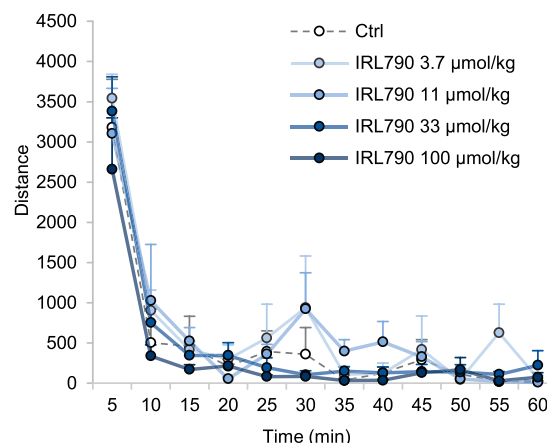


**Fig. 1.** Effects of IRL790 on spontaneous locomotor activity. Shown are means  $\pm$  S.E.M. of total distance traveled over 5-minute intervals throughout the 60-minute recording session, expressed in arbitrary length units. IRL790 (3.7, 11, 33, or 100  $\mu\text{mol/kg}$ , s.c.) was administered subcutaneously 4' before the start of recording. Controls received saline.  $N = 4/\text{group}$ . There was a significant effect of time ( $P < 0.00001$ ) but no significant effect of treatment or time  $\times$  treatment (repeated measures ANOVA). Ctrl, control.

$P < 0.000001$ ; treatment  $F(1,12) = 48.1$ ,  $P = 0.00002$ ; time  $\times$  treatment  $F(6,72) = 11.8$ ,  $P < 0.000001$ , adjusted  $P = 0.000006$ ]. Post hoc testing indicated significant effects at 10 mg/kg,  $P = 0.0021$ , and 20 mg/kg,  $P = 0.000024$ . Statistical significance was confirmed with nonparametric testing, showing a significant effect at 10 mg/kg,  $P = 0.017$  versus controls, and at 20 mg/kg,  $P = 0.002$  versus controls. At the highest dose, L-DOPA-induced rotation was slightly increased in the L-DOPA + IRL790-treated group, suggesting that the antidyskinetic effect of IRL790 did not reduce the beneficial L-DOPA-induced motor activation (Fig. 6). Taken together, combining the two experimental sessions covering the dose range 1–20 mg/kg (3.2–64  $\mu\text{mol/kg}$ ) s.c., a dose-dependent reduction of LIDs was observed with an  $\text{ED}_{50}$  of  $\sim 4$  mg/kg

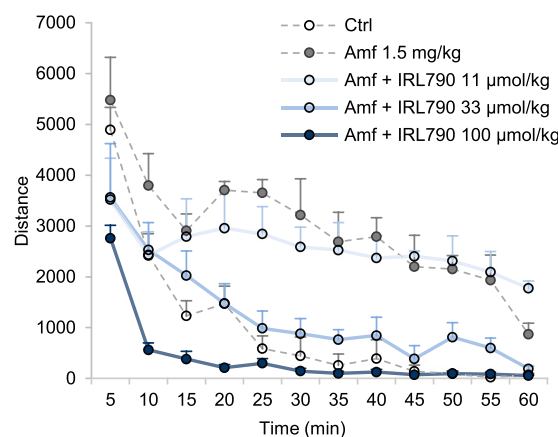


**Fig. 2.** Effects of IRL790 on D-amphetamine-induced hyperactivity. Shown are means  $\pm$  S.E.M. of total distance traveled over 5-minute intervals throughout the 60-minute recording session, expressed in arbitrary length units. D-amphetamine (1.5 mg/kg, i.p.) was administered 10' before the start of recording, and IRL790 (3.7, 11, 33, or 100  $\mu\text{mol/kg}$ , s.c.) was administered 4' before the start of recording. Controls received saline.  $N = 4/\text{group}$ . IRL790 significantly reduced D-amphetamine-induced hyperactivity at 33 and 100  $\mu\text{mol/kg}$  ( $P < 0.001$ , repeated measures ANOVA, post hoc Dunnett's test).

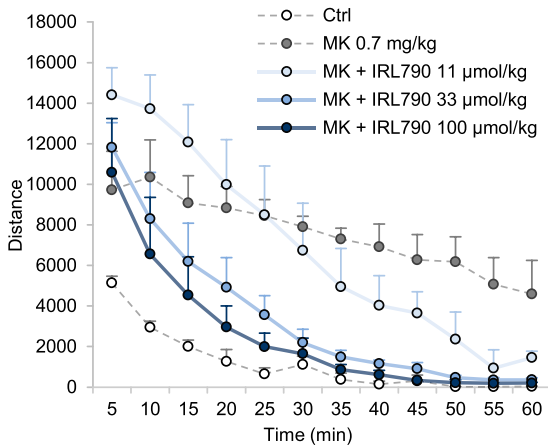


**Fig. 3.** Effects of IRL790 on MK-801-induced hyperactivity. Shown are means  $\pm$  S.E.M. of total distance traveled over 5-minute intervals throughout the 60-minute recording session, expressed in arbitrary length units. MK-801 (0.7 mg/kg, i.p.) was administered 90' before the start of recording, and IRL790 (3.7, 11, 33, and 100  $\mu$ mol/kg, s.c.) was administered 4' before the start of recording. Controls received saline.  $N = 4$ /group. IRL790 significantly reduced MK-801-induced hyperactivity at 33 ( $P < 0.05$ ) and 100 ( $P < 0.01$ )  $\mu$ mol/kg (repeated measures ANOVA, post hoc Dunnett's test).

(13  $\mu$ mol/kg; Fig. 7), with a reduction by 40%–50% in the total composite AIMS score as compared with the control group at 10 and 20 mg/kg.

### Effects on Neurochemistry and IEGs

Ex vivo neurochemical analysis of brain tissue revealed dose-dependent effects on monoaminergic indices, in particular DOPAC and HVA, reaching approximately 250%–300% relative to control group means at the highest dose (100  $\mu$ mol/kg) in all three brain structures sampled, suggesting increased dopamine metabolism across brain regions (Fig. 8). There were also decreases in cortical NA and DA at the top dose (reduced to 80% and 85% of control mean, respectively,  $P < 0.05$ ) and in striatal DA at 33 and 100  $\mu$ mol/kg (83%,  $P < 0.05$  and 78%,  $P < 0.001$ , respectively, relative to controls).

Neurochemical effects were also assessed by in vivo brain microdialysis, capturing monoamine analytes and ACh in extracellular fluid in conscious, freely moving rats. Dialysates were collected from the striatum and the prefrontal cortex for 3 hours after the administration of IRL790 at 16.7 or 50  $\mu$ mol/kg s.c. and assessed with respect to monoaminergic neurochemical indices. In a separate microdialysis study, ACh levels were monitored in prefrontal cortex, ventral hippocampus, and striatum after IRL790 50  $\mu$ mol/kg s.c. or saline. IRL790 elicited dose-dependent increases in extracellular levels of NA and DA (Fig. 9) as well as the DA metabolites DOPAC and HVA (data not shown). At 50  $\mu$ mol/kg, prefrontal cortex DA increased to 200% of baseline, and striatal DA reached 270% of baseline. NA increased to 130% of baseline in the prefrontal cortex and 270% of baseline in the striatum. Repeated measures ANOVA indicated a significant effect of time [ $F(9,117) = 9.46$ ,  $P < 0.000001$ ] and time  $\times$  treatment [ $F(18,117) = 2.57$ ,  $P = 0.001$ ] for DA in the prefrontal cortex; a significant effect of time [ $F(9,126) = 15.44$ ,  $P < 0.0000001$ ], treatment [ $F(2,14) = 17.96$ ,  $P = 0.0001$ ], and time  $\times$  treatment of DA in the striatum [ $F(18,126) = 5.67$ ,  $P < 0.0000001$ ]; and

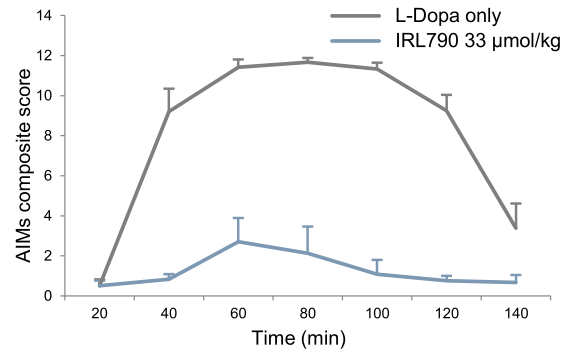


**Fig. 4.** Effects of IRL790 in the AIMS model in-house study. Rats were subjected to unilateral 6-OHDA lesion followed by 3 weeks of treatment with L-DOPA, 6.5 mg/kg dose s.c. (plus benserazide 12 mg/kg), to establish full expression of dyskinesias. On the test day, IRL790 (33  $\mu$ mol/kg, s.c.) was administered together with L-DOPA (6.5 mg/kg, s.c.) ( $n = 6$ ). Controls received L-DOPA only ( $n = 6$ ). Groups were balanced to have similar AIMS scores at baseline. Shown are means  $\pm$  S.E.M. of composite AIMS scores, measured at 20-minute intervals. IRL790 resulted in a near-complete suppression of dyskinesia, which was statistically significant (effect of treatment,  $P < 0.000001$ , repeated measures ANOVA;  $P < 0.01$ , Mann-Whitney  $U$  test, based on total composite scores).

a significant effect of time [ $F(9,63) = 3.08$ ,  $P < 0.004$ ] and time  $\times$  treatment of NA in the striatum [ $F(18,63) = 2.49$ ,  $P = 0.004$ ]. There was no significant effect on 5-HT in either region. Levels of ACh were increased across brain regions, reaching 329% of baseline in the pfc and 225% of baseline in the ventral hippocampus (Fig. 10). Repeated measures ANOVA indicated a significant effect of time [ $F(9,90) = 12.37$ ,  $P < 0.000001$ ], treatment [ $F(1,10) = 33.14$ ,  $P = 0.0002$ ], and time  $\times$  treatment

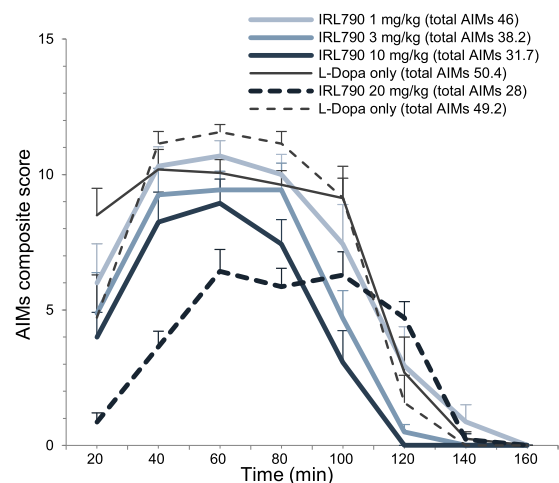


**Fig. 5.** Effects of IRL790 in AIMS model, external study. Rats were subjected to unilateral 6-OHDA lesion followed by 4 weeks of treatment with L-DOPA (6.5 mg/kg dose, s.c.) plus benserazide (12 mg/kg, s.c.) to establish full expression of dyskinesias. On the test day, IRL790 (1, 3, or 10 mg/kg, s.c.) was administered 20' before L-DOPA (6.5 mg/kg, s.c.) ( $n = 8$ ). Controls received L-DOPA only ( $n = 8$ ). In a separate experimental session, L-DOPA + IRL790, 20 mg/kg, was tested ( $n = 7$ /group). All groups were balanced to have similar AIMS scores at baseline. Shown are means  $\pm$  S.E.M. of composite AIMS scores, measured at 20-minute intervals. Data from the separate experimental session testing IRL790 (20 mg/kg) are represented with dashed lines. IRL790 resulted in a dose-dependent suppression of dyskinesia, which was statistically significant at 10 and 20 mg/kg ( $P < 0.01$ ;  $P < 0.0001$ , respectively; repeated measures ANOVA followed by Dunnett's test, confirmed with Mann-Whitney  $U$  test, based on total composite scores,  $P < 0.05$ ;  $P < 0.01$  at 10 and 20 mg/kg, respectively).

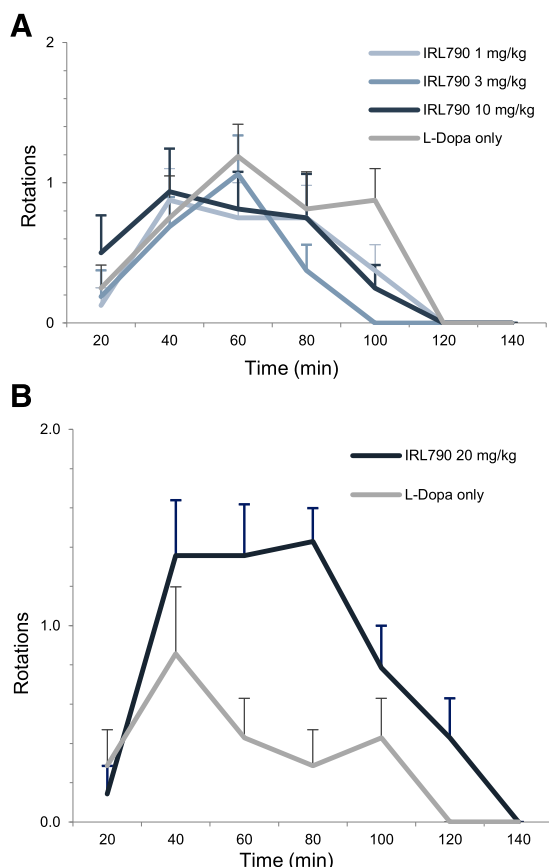


**Fig. 6.** Effects of IRL790 on rotations in AIMs model, external study. Rats were subjected to unilateral 6-OHDA lesion followed by 4 weeks of treatment with L-DOPA (6.5 mg/kg dose, s.c.) plus benserazide (12 mg/kg) to establish full expression of dyskinesias. On the test day, IRL790 was administered at 1, 3, and 10 mg/kg  $\mu$ mol/kg s.c. 20' before L-DOPA (6.5 mg/kg, s.c.) ( $n = 8$ ). Controls received L-DOPA only ( $n = 8$ ). In a separate experimental session (lower panel), L-DOPA + IRL790, 20 mg/kg, was tested ( $n = 7$ /group). All groups were balanced to have similar AIMs scores at baseline. Shown are means  $\pm$  S.E.M. of rotations, measured at 20-minute intervals, with data from the first experimental session testing 1–10 mg/kg in the upper panel and data from the experimental session testing IRL790 20 mg/kg in the lower panel. IRL790 did not display any reduction of the rotational response to L-DOPA.

[ $F(9,90) = 4.85$ ,  $P = 0.00003$ ] in the pfc as well as in the ventral hippocampus (time [ $F(9,36) = 4.45$ ,  $P = 0.0006$ ], treatment [ $F(1,4) = 18.5$ ,  $P = 0.013$ ], time  $\times$  treatment [ $F(9,36) = 2.26$ ,  $P = 0.040$ ]).

Effects on IEG mRNA are shown in Fig. 11. IRL790 dose-dependently and potently increased *Arc* in the striatum, reaching 241% ( $P < 0.01$ ), 329% ( $P < 0.001$ ), and 384% ( $P < 0.001$ ) versus vehicle controls at 11, 33, 100  $\mu$ mol/kg, respectively. *Arc* was also significantly increased at 11–100  $\mu$ mol/kg in the frontal cortex and in the limbic region, reaching 153%–162% of control in the frontal cortex and 166%–186% of control in the limbic region (Fig. 10). *Cfos*, *homer*, and *egr* were increased in the striatal and limbic regions. *NPAS4* was increased in the striatum. As with *Arc*, the effects on *cfos*, *homer*, *egr*, and *NPAS4* were generally potent, reaching statistical significance even at the lowest dose tested (11  $\mu$ mol/kg), with particularly large magnitudes for striatal *cfos*, *homer*, and *NPAS4* (300%–800% of control means at the top dose). There were also minor effects on *Nptx2*;

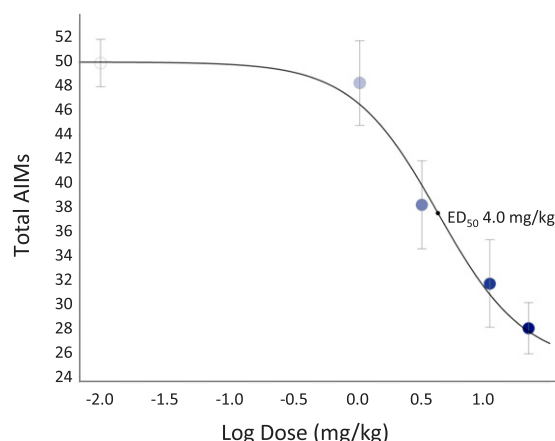


**Fig. 7.** Dose-response analysis of total AIMs score. Graph based on data from external study (IRL790 1, 3, 10, and 20 mg/kg, and controls). Controls are drawn at log (dose) =  $-2$ .  $N = 7$  to 8/dose. Shown are means  $\pm$  S.E.M.  $ED_{50} = 4$  mg/kg (black circle) was estimated by means of fitting a sigmoidal curve (Hill equation), assuming  $E_{min} = 50$  (no reduction) and  $E_{max} = 25$  (50% reduction of AIMs).

however, these were of small magnitude and with no consistent dose-response pattern: small increases were observed in the striatum at 33 and 100  $\mu$ mol/kg (30%–50% increase vs. controls), and a slight decrease was observed in the frontal cortex (around 20% decrease vs. controls at 11 and 33  $\mu$ mol/kg).

For the gene map, IEG expression data on 13 compounds were analyzed using PLS regression, as described previously (Waters et al., 2017). A five-component model was obtained, describing 72% of the variance in the X-block ( $R^2X$ ) and 26% of the variance in the Y-block ( $R^2Y$ ),  $Q^2_{cum} = 0.184$ .  $w^*c$  loadings (X and Y variable loading weights) for the two first components are shown in Fig. 12. This type of plot shows clusters among the compounds studied, along with underlying effect patterns in the variables measured. Compounds located close

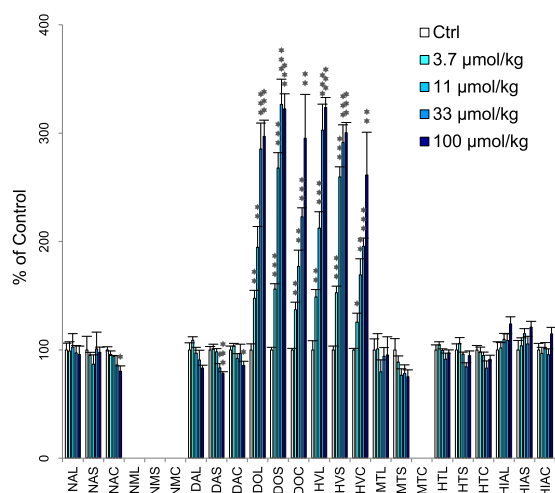


**Fig. 8.** Effects of IRL790 on ex vivo monoaminergic neurochemistry. Analyte is denoted as follows: DA, dopamine; DO, DOPAC; HIA, 5-HIAA; HT, 5-HT; HV, HVA; MT, 3-MT; NA, norepinephrine; NM, normetanephrine. Brain region: C, cortex; L, limbic region; S, striatum. Brains were removed and dissected 60' after administration of IRL790 (3.7, 11, 33, or 100  $\mu$ mol/kg, s.c.). Controls (Ctrl) received saline.  $N = 4$ . Shown are means  $\pm$  S.E.M., expressed as percentage of control group mean. \* $P < 0.05$ ; \*\* $P < 0.01$ .  $P < 0.001$  vs. control group, Student's  $t$  test.



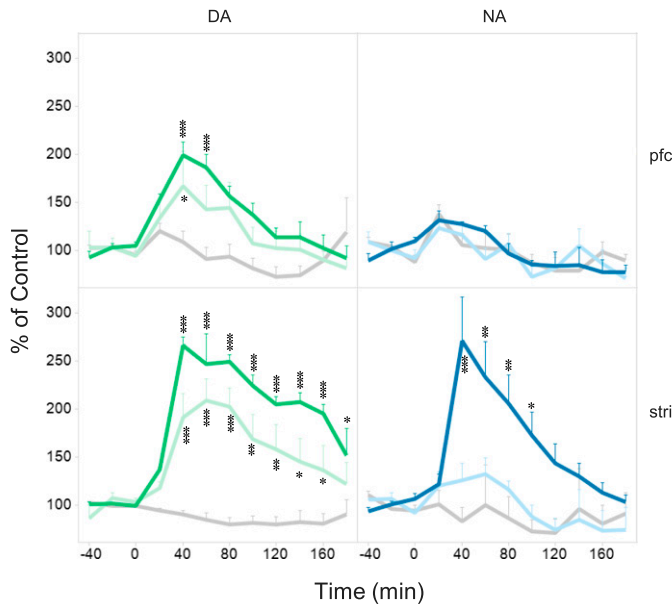


**Fig. 9.** Effects of IRL790 on rat brain regional dialysate levels of monoamines. Dialysate levels of DA and NA in the prefrontal cortex (upper panel) and striatum (stri, lower panel) were monitored 0–180 minutes after administration of IRL790 (16  $\mu\text{mol/kg}$ , light blue; 50  $\mu\text{mol/kg}$ , dark blue). Shown are the mean dialysate levels/20-minute sample  $\pm$  S.E.M., expressed as percentage of baseline values (avg. of the three fractions collected 40–0 minutes before dosing).  $N = 5$ –7/group (NA striatum, 16  $\mu\text{mol/kg}$ ,  $n = 2$ ). Significant differences between effect of vehicle and IRL790 at specific time points are indicated as follows: \* $P < 0.05$ ; \*\* $P < 0.01$ ; \*\*\* $P < 0.001$  (repeated measures ANOVA, followed by Fischer's Least Significant Difference post hoc test).

to each other in the plot tend to share gene expression patterns, whereas diametrically opposing positions indicate opposing effects. For the variable  $w^*$  loadings, clustering indicates covariance, and diametrically opposing positions reflect negative correlations. Positions in orthogonal directions indicate independent effects. In this model, the first component ( $x$ -axis) essentially represents overall increase (left) or decrease (right) across IEGs, whereas component 2 ( $y$ -axis) captures regional differences (increase in striatal region downward, cortical regions upward). There is a clustering of antipsychotic compounds in the lower-right quadrant, reflecting a shared feature of general decreases in IEGs, along with a tendency to increase striatal Arc and cfos (downward direction in plot). Antiparkinsonian agents (ropinirole, amantadine) display weak effects, decreasing striatal IEGs, and for ropinirole in particular, increases in cortical IEGs such as NPAS4 and cfos. Apomorphine, donepezil, and memantine all display more-pronounced increases in cortical/hippocampal IEGs but fewer effects on striatal IEGs. IRL790 displays a distinct pattern, with increases both in striatal, limbic, and cortical IEGs, in particular Arc, resulting in an intermediate position between antipsychotics and the DA D1 agonist dihydroxidine.

### In Vitro Pharmacology

In vitro binding characteristics of IRL790 were assessed in a broad radioligand binding screen, followed by determination of  $\text{IC}_{50}/K_i$  values at selected targets, at which at least 20% inhibition of control specific binding was observed (Table 1).

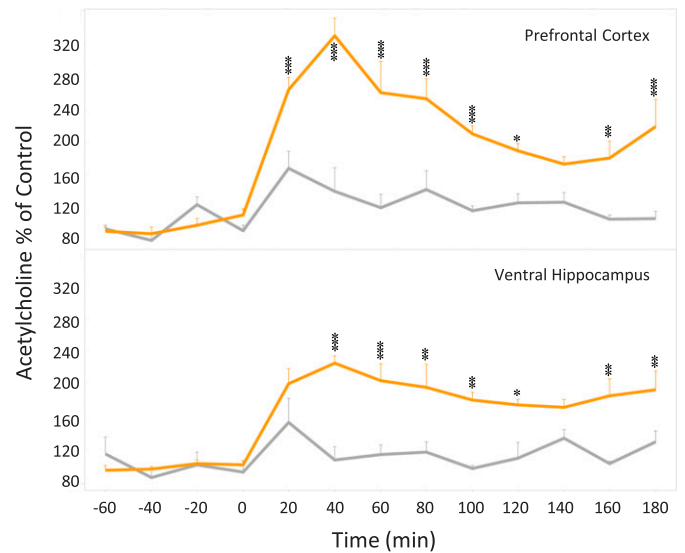


**Fig. 10.** Effects of IRL790 on rat brain regional dialysate levels of ACh. Dialysate levels of ACh in the prefrontal cortex (upper panel) and ventral hippocampus (lower panel) were monitored 0–180 minutes after administration of IRL790, 50  $\mu\text{mol/kg}$ , or vehicle (saline). Shown are the mean dialysate levels/20-minute sample  $\pm$  S.E.M., expressed as percentage of baseline values (avg. of the four fractions collected 60–0 minutes before dosing).  $N = 6$ /group, pfc; 3 to 4/group, ventral hippocampus. Significant differences between effect of vehicle and IRL790 at specific time points are indicated as follows: \* $P < 0.05$ ; \*\* $P < 0.01$ ; \*\*\* $P < 0.001$  (repeated measures ANOVA, followed by Fischer's Least Significant Difference post hoc test).

IRL790 displayed moderate affinity across a range of receptors, enzymes, and transporters (Table 1). At the primary target, the dopamine D3 receptor, IRL790 had a  $K_i$  of 90 nM. Sub-micromolar affinities were also measured at DA D2 and

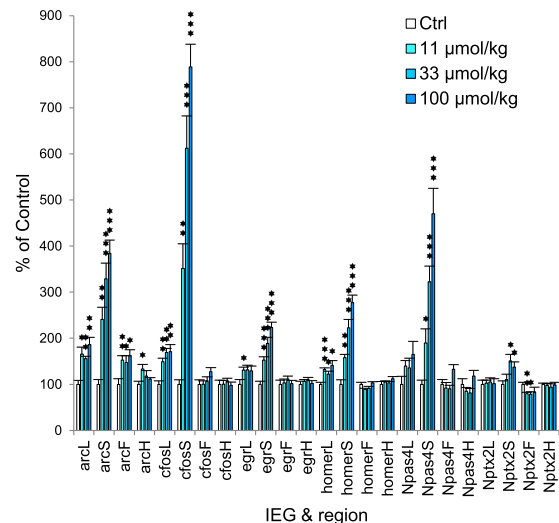


**Fig. 11.** Effects of IRL790 on expression of IEGs. Brains were removed and dissected 65' after administration of IRL790 at 11, 33, and 100  $\mu\text{mol/kg}$ , s.c. Controls received saline. Brain region: F, frontal cortex; L, limbic region; S, striatum. Arc (activity-related cytoskeletal protein), c-Fos (cellular DNA-binding proteins encoded by the c-Fos genes), EGR1, Homer1 (a postsynaptic density adaptor protein), NPAS4, and Nptx2 were measured by quantitative PCR. Results are presented as percentage of controls (means  $\pm$  S.E.M.;  $n = 5$  animals/treatment group). Statistics: Student's  $t$  test (two-tailed), \* $P < 0.05$ ; \*\* $P < 0.01$ ; \*\*\* $P < 0.001$  vs. controls. Data are sorted by gene, then by region, and then by ascending dose from left to right. Ctrl, control.

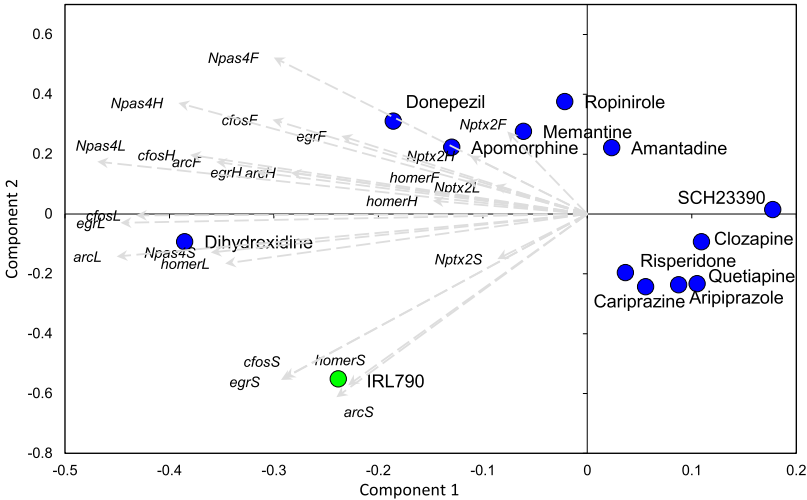


**Fig. 12.** Gene expression map on IRL790 and selected compounds implicated in PD. Shown are w\*c loadings, component 1 vs. component 2, from a PLS regression model of effects on IEGs (independent variable block) vs. treatment with different test compounds (dependent variable block of discriminant variables denoting treatment). Loadings indicate correlation patterns among variables (w\* loadings) and effect patterns and clusters among compounds (c loadings). Compounds located close to each other share major effect patterns, whereas diametrically opposing positions reflect opposing effects. Variable loadings indicate effects governing mapping of compounds. Variables located close to each other tend to be correlated, whereas diametrically opposing positions reflect negative correlations. Variables located in orthogonal directions are uncorrelated.

σ1 receptors, and micromolar affinities were measured at 5-HT1a, 5-HT2a, and 5-HT7 receptors. IRL790 was further investigated in vitro in assays designed to detect intrinsic activity in cellular functional assays at human recombinant D2S, D3, and serotonergic receptors (see Table 2). IRL790 did not show any agonist-like properties at D2, D3, 5-HT2, or 5-HT7 receptors. The compound displays weak partial agonist properties at 5-HT1A receptors, albeit with an EC<sub>50</sub> > 100 μM.

IRL790 was also tested for antagonist properties in in vitro cellular assays with human recombinant receptors. Antagonist properties at DA D2S, 5-HT1A, and 5-HT2A receptors were observed; see Table 3.

Computational Docking Studies

Figure 13 shows the best-scoring binding pose for IRL790 in the crystal structure of the dopamine D3 receptor (Chien et al., 2010). IRL790 binds in a horizontal orientation with reference to the vertically oriented transmembrane helices. The methyl sulfone moiety of IRL790 points toward the serine residues Ser192 and Ser193 (S<sup>5.42</sup> and S<sup>5.43</sup> using Ballesteros-Weinstein numbering (Ballesteros and Weinstein, 1995) in the transmembrane helix 5 (TM5), and the basic amine interacts with the aspartic acid residue Asp110 (D<sup>3.32</sup>) in TM3. These conserved residues among monoaminergic G-protein-coupled receptors are known to be key interaction residues for receptor agonists (Malo et al., 2012). Thus, the modeling results indicate that IRL790 preferably binds in a typical agonist-like binding mode. The best-scoring binding pose for IRL790 in the structure model of the dopamine D2 receptor is in essence similar to the best D3

pose, but the internal conformational energy of IRL790 is higher, and the docking score slightly worse, for the D2 pose. The only sequence position in the binding site region that differs between the D2 and D3 receptors is in the second extracellular loop (ECL2) at the C + 1 (Conner et al., 2007) position, i.e., the position after the conserved cysteine residue making a disulfide bridge to TM3, which is close to the binding pocket entrance (see Fig. 14). The D3 receptor has a serine pointing away from the ligand (IRL790) in the crystal structure, and the D2 receptor has a bulkier isoleucine amino acid that is pointing toward the ligand and causing the entrance to be narrower in the D2 structure model.

Discussion

IRL790 was developed with the aim to create an antidyskinetic and antipsychotic compound that exerts its pharmacological effects through interactions with DA D3/D2 type receptors. The underlying design strategy was to use full or partial dopamine receptor agonists and modify their pharmacological properties away from agonism toward antagonism without following the conventional route of increasing size and lipophilicity. Given that agonists of DA D3/D2 receptors tend to be smaller, more hydrophilic molecules, whereas antagonists are usually larger and more lipophilic (Malo et al., 2010; Li et al., 2016), we speculated that this approach could yield DA D3/D2 antagonists that mimic the specific interactions of DA (i.e., active state of the receptor) better than large, lipophilic antagonists, which bind to and stabilize the inactive state of the receptor (Goddard and Abrol, 2007), with slow

TABLE 3  
Antagonist effects in cellular functional assays (human receptors)

Assay	IC <sub>50</sub>	K <sub>B</sub>	Stimulus	Source	Measured Component	Reference
D2S	13 μM	0.87 μM	Dopamine (30 nM)	HEK-293 cells	Impedance	SOP 1C531
D3	9.8 μM	2.3 μM	Dopamine (10 nM)	CHO cells	cAMP	SOP 1C374
5-HT1A	n.c. <sup>a</sup>		8-OH-DPAT (100 nM)	HEK-293 cells	Impedance	SOP 1C913
5-HT2A	n.c.		Serotonin (100 nM)	HEK-293 cells	IP <sub>1</sub>	SOP 1C865

n.c., not calculable; SOP, standard operating procedures used by Cerep.  
<sup>a</sup>IC<sub>50</sub> not calculable due to lack of effect. IP1, inositol mono-phosphate. 8-OH-DPAT, 8-hydroxy-2-(di-N-propylamino)tetralin.

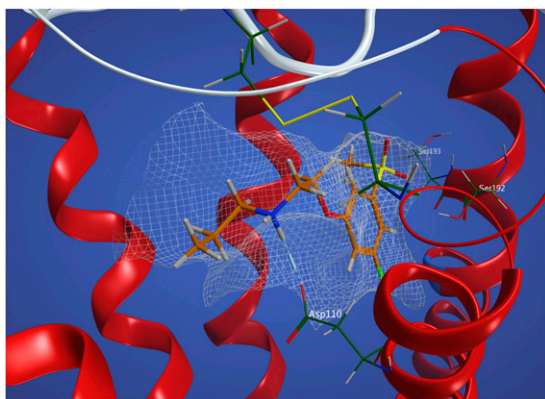


**Fig. 13.** IRL790 docked into the binding site of the dopamine D3 receptor crystal structure (PDB entry 3pbl). A ribbon representation of the receptor with three key residues important for agonist binding and the disulfide bridge between ECL2 and TM3 is shown. The shape of the binding site is illustrated by the accessible surface for the parts of the protein that are in close proximity to the ligand, represented by a white mesh showing how close an oxygen atom in a water molecule could be to the protein surface without any steric repulsion.

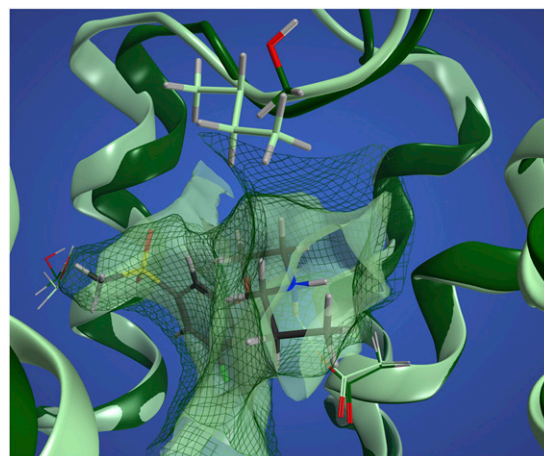


**Fig. 14.** An overlay of the binding sites of the dopamine D3 receptor crystal structure (dark green) and the homology model of the dopamine D2 receptor (light green). A ribbon representation of the receptor with the only residue position in ECL2 (C + 1) with a mutation in the binding site (Ile in D2 and Ser in D3) is shown with thick bond representation. Other key residues (Asp<sup>3.32</sup> in TM3 and Ser<sup>5.42</sup> and Ser<sup>5.43</sup> in TM5) are shown with thin bond representations. The difference in shape of the binding sites are illustrated by the accessible surface for the parts of the protein that are in close proximity to the ligand (D3 with a mesh and D2 with a solid surface representation).

receptor dissociation (Tresadern et al., 2011). We hypothesized that such a dopamine antagonist with physicochemical properties similar to agonists would exert antidyskinetic and antipsychotic effects in states of dysregulated dopaminergic signaling, while having little negative impact on physiologic dopamine transmission and, hence, minimal liability for motor side effects. This prediction was, to a large extent, manifested in IRL790's *in vivo* pharmacological profile. The starting point for discovery and development of IRL790 was a series of 2-(aminomethyl)-chromans (Mewshaw et al., 1997) as partial DA D2 agonists with varying intrinsic activity. By careful modification of key elements important for intrinsic activity, a series of compounds with DA D3/D2 receptor antagonist properties were discovered, among which IRL790, a small, hydrophilic compound (calculated octanol/water partition coefficient/clogP = 1.59, mol. wt. = 275.3), was selected for further development. The *in vivo* test battery was performed in male rats, except for the external AIMs study, in which female rats were used.

IRL790 displays a neurochemical signature with effects indicating increased dopamine metabolism across brain regions. In line with the effects on *ex vivo* monoaminergic neurochemistry, *in vivo* microdialysis showed increases in extracellular levels of NA and DA in the frontal cortex and the striatum. Similar profiles have been observed with atypical antipsychotics, attributable to dopamine receptor antagonism, known to produce increases in DOPAC and HVA (Carlsson and Lindqvist, 1963; Magnusson et al., 1986), in combination with interactions at 5-HT1a, 5-HT2a, 5-HT7, or  $\alpha$ 2 receptors, proposed to result in enhanced release of dopamine (Alex and Pehek, 2007; Wesolowska and Kowalska, 2008; Marcus et al., 2010). IRL790 also increased extracellular levels of ACh in the pfc and hippocampus, an effect observed with DA D3 antagonists and some atypical, but not typical, antipsychotics (Lacroix et al., 2006). The gene expression profile also shares some features with antipsychotics. *Arc* is an immediate early gene triggered by, e.g., synaptic NMDA receptor activation (Bramham et al., 2010). It is involved in consolidation of memory and related processes, such as long-term potentiation, and is a key regulator of synaptic plasticity.

*Cfos*, encoding a transcription factor, is a more nonspecific marker of neuronal activation (de Bartolomeis et al., 2017). The dose-dependent increase of striatal *Arc* and *cfos* is a common feature of dopamine D2 antagonists (Robbins et al., 2008; Fumagalli et al., 2009; Waters et al., 2014; de Bartolomeis et al., 2017), proposedly linked to antagonism at DA D2 heteroreceptors at glutamatergic corticostriatal terminals, leading to enhanced synaptic NMDA-mediated signaling onto striatal neurons (Waters et al., 2014). With IRL790, we also see dose-dependent increases of *Nptx*, *NPAS*, *egr*, and *homer* in the striatum, likely reflecting downstream effects of the modulation of synaptic activity in striatal neurons. The increase in frontal cortex *Arc*, on the other hand, is not shared by dopamine antagonists, which generally decrease this biomarker upon acute administration (Waters et al., 2014; de Bartolomeis et al., 2017). Enhanced cortical ACh may contribute to this cortical *Arc* increase (Teber et al., 2004). The gene map provides a comparative overview of IEG expression patterns for a set of compounds relevant for the PD population. The IEG profile of IRL790 is reflected in a position in the map representing both features shared with antipsychotics, as discussed above, and features unique to IRL790, e.g., increases in frontal and limbic IEGs (*Arc*, *cfos*, *NPAS4*). This profile is distinct from the other classes represented in the model, including cariprazine, a novel antipsychotic described as a DA D3-receptor–preferring versus D2-receptor–preferring partial agonist (Garnock-Jones, 2017) that is more akin to other antipsychotics in its IEG expression profile. Moreover, IRL790 displays antagonist properties at the D3 receptor and, thus, differs from cariprazine, which is a high-affinity partial agonist at these sites. This notwithstanding, IRL790 paradoxically displays an agonist-like receptor binding mode (see docking studies below). Taken together, the binding properties imply a different interplay with the endogenous ligand at D3 receptors as compared with cariprazine, in turn likely influencing downstream effects measured *in vivo*, including

IEGs. IRL790 is also distinct from compounds used in dementia, which generally show their most prominent IEG increases in frontal cortex and hippocampus, with less impact on striatal IEGs.

The effects of IRL790 on locomotor activity in rodents were studied in several models. There was no effect on spontaneous locomotor activity over a dose range eliciting significant effects on neurochemical and gene biomarkers. In contrast, IRL790 reduced locomotor hyperactivity elicited by pretreatment with either D-amphetamine or MK-801, demonstrating the ability to normalize the behavioral phenotype in hyperdopaminergic as well as hypoglutamatergic states.

Balancing effects on aberrant motor phenotypes were also evident in the investigations made using the rodent 6-OHDA AIMs model. This model is considered to have predictive validity for evaluation of antidyskinetic efficacy of new therapies (Iderberg et al., 2012). IRL790 dose-dependently reduced AIMs, and this alleviation of involuntary movements was not achieved at the cost of any impairment of the motor effects of L-DOPA as such, in this study captured as rotational response to L-DOPA. It should be noted that such rotations are a complex phenomenon, not solely representing antiparkinsonian effects of L-DOPA; however, the lack of reduction of rotations appears consistent with the lack of general inhibition of locomotor activity by IRL790. At the highest dose of IRL790, rotational behavior even appeared somewhat enhanced.

In vitro, sub-micromolar affinities were observed at DA D3, D2, and  $\sigma$ 1 receptors, and micromolar affinities were observed at 5-HT1a, 5-HT2a, and 5-HT7 receptors. Functional in vitro studies showed no intrinsic activity at the receptors studied, except at 5-HT1A receptors, in which a partial agonist effect at high concentrations,  $EC_{50} \approx 100 \mu\text{M}$ , was detected. Additional functional studies confirmed antagonist actions of IRL790 at DA D3 and D2, 5-HT1a, and 5-HT2a receptors. The highest affinity was found at DA D3, followed by D2 (6- to 8-fold less) receptors.

Dopamine D3 receptors are clearly implicated in the pathogenesis of LIDs, in which they are hypothesized to mediate aberrant dopamine D1 receptor signaling through the formation of D1-D3 receptor dimers (Solís and Moratalla, 2018). Hence, D3 receptor antagonism has been suggested as an attractive target for pharmacological alleviation of LIDs. Peak plasma concentrations of IRL790, reported from a clinical PD-LIDs study, around 220 nM are consistent with pharmacologically relevant interactions at DA D3 receptors in the suggested therapeutic dose range (Svenningsson et al., 2018).

D3/D2 receptors are also implicated in psychosis treatment, with most therapeutic agents being D2-preferring receptor antagonists or partial agonists. Interestingly, the D3/D2 preference ratio displayed by IRL790 is similar to that reported for the recently launched partial DA receptor agonist cariprazine, which has shown broad antipsychotic effectiveness (Garnock-Jones, 2017; Nemeth et al., 2017; Fleischacker et al., 2019). IRL790 is less potent at D3 receptors than cariprazine but is nonetheless within the same nanomolar affinity range as the endogenous transmitter DA itself for this site (Kiss et al., 2010; Stahl, 2017). IRL790 would therefore be expected to effectively compete with DA for the D3 receptors in vivo at exposures attained under the conditions reported in this paper. Computational docking studies of

IRL790 into the ligand binding site of dopamine D3 and D2 receptor structures confirm the design idea of this new type of dopaminergic antagonist with an agonist-like binding mode (Fig. 13). The methyl sulfone moiety of IRL790 does not interact with the serine residues in TM5 in the same way as the typical catechol moiety in agonists does. This may explain the lack of intrinsic activity observed for IRL790. Shape differences in the entrance region of the ligand may explain the differences in docking scores and ligand conformational energies observed when docking IRL790 into dopamine D3 versus D2 receptor models. The combination of an agonist-like binding mode of IRL790 and the subtle difference in the shape of the binding sites of the D3 and D2 receptors is consistent with the moderate in vitro D3 binding affinity and the D3 versus D2 preference observed.

In summary, IRL790 displays an in vivo pharmacological effect pattern, with reduction of AIMs in the rodent 6-OHDA lesion model, and antipsychotic-like effects in validated pharmacological models, without negatively impacting normal motor performance. The in vivo profile, including neurochemical and IEG responses, suggesting modulation of DA neurotransmission, is consistent with the in vitro pharmacology, suggesting DA D3 receptors as a primary site of action. Computational docking at DA D3 receptors supports preferential affinity at DA D3 receptors with an agonist-like binding mode. This said, the precise extent to which the DA D3, D2, and other target sites contribute to the overall profile of IRL790 remains to be further established. The in silico, in vitro, and in vivo properties of IRL790 reflect the design principle applied in the drug discovery process, in which we sought to obtain antagonist compounds with an agonist-like structural motif to softly modulate endogenous neurotransmission in such a way that normal dopaminergic functions are left intact, whereas motor and psychiatric disturbances related to aberrations in dopaminergic transmission are alleviated. This strategy, we believe, is a key factor in the favorable clinical efficacy and tolerability profile of IRL790, even in the very sensitive population of patients with advanced Parkinson disease (Svenningsson et al., 2018).

#### Acknowledgments

Anna Carin Jansson is acknowledged for analyzing acetylcholine in microdialysis samples.

#### Authorship Contributions

*Participated in research design:* S. Waters, Sonesson, Svensson, Tedroff, Carta, Ljung, Gunnergren, Hjorth, N. Waters.

*Conducted experiments:* Carta, Ljung, Gunnergren, Edling, Svanberg, Fagerberg.

*Performed data analysis:* S. Waters, Svensson, Ljung, Gunnergren, Edling, Svanberg, Fagerberg, Kullingsjö.

*Wrote or contributed to the writing of the manuscript:* S. Waters, Sonesson, Svensson, Tedroff, Carta, Ljung, Gunnergren, Edling, Svanberg, Fagerberg, Kullingsjö, Hjorth, N. Waters,

#### References

- Ahlskog JE and Muentner MD (2001) Frequency of levodopa-related dyskinesias and motor fluctuations as estimated from the cumulative literature. *Mov Disord* **16**: 448–458.
- Alex KD and Pehek EA (2007) Pharmacologic mechanisms of serotonergic regulation of dopamine neurotransmission. *Pharmacol Ther* **113**:296–320.
- Ballesteros JA and Weinstein H (1995) Integrated methods for the construction of three-dimensional models and computational probing of structure-function relations in G protein-coupled receptors, in *Methods in Neurosciences* (Sealfon SC 366–428, Academic Press, San Diego, CA.



- Bézard E, Ferry S, Mach U, Stark H, Leriche L, Boraud T, Gross C, and Sokoloff P (2003) Attenuation of levodopa-induced dyskinesia by normalizing dopamine D3 receptor function. *Nat Med* **9**:762–767.
- Bordet R, Ridray S, Carboni S, Diaz J, Sokoloff P, and Schwartz JC (1997) Induction of dopamine D3 receptor expression as a mechanism of behavioral sensitization to levodopa. *Proc Natl Acad Sci USA* **94**:3363–3367.
- Borgkvist A, Lieberman OJ, and Sulzer D (2018) Synaptic plasticity may underlie l-DOPA induced dyskinesia. *Curr Opin Neurobiol* **48**:71–78.
- Bramham CR, Alme MN, Bittins M, Kuipers SD, Nair RR, Pai B, Panja D, Schubert M, Soule J, Tiron A, et al. (2010) The Arc of synaptic memory. *Exp Brain Res* **200**: 125–140.
- Carlsson A and Lindqvist M (1963) Effect of chlorpromazine or haloperidol on formation of 3-methoxytyramine and normetanephrine in mouse brain. *Acta Pharmacol Toxicol (Copenh)* **20**:140–144.
- Cenci A and Lundblad M (2005) Utility of 6-Hydroxydopamine lesioned rats in the preclinical screening of novel treatments for Parkinson's disease. *Animal Models of Movement Disorders* pp 193–208, Elsevier Academic Press, San Diego, CA.
- Cenci MA (2014) Presynaptic mechanisms of l-DOPA-induced dyskinesia: the findings, the debate, and the therapeutic implications. *Front Neurol* **5**:242.
- Chien EY, Liu W, Zhao Q, Katritch V, Han GW, Hanson MA, Shi L, Newman AH, Javitch JA, Cherezov V, et al. (2010) Structure of the human dopamine D3 receptor in complex with a D2/D3 selective antagonist. *Science* **330**:1091–1095.
- Chomczynski P and Sacchi N (1987) Single-step method of RNA isolation by acid guanidinium thiocyanate-phenol-chloroform extraction. *Anal Biochem* **162**: 156–159.
- Conner M, Hawtin SR, Simms J, Wootten D, Lawson Z, Conner AC, Parslow RA, and Wheatley M (2007) Systematic analysis of the entire second extracellular loop of the V(1a) vasopressin receptor: key residues, conserved throughout a G-protein-coupled receptor family, identified. *J Biol Chem* **282**:17405–17412.
- Cote SR, Chitravanshi VC, Bleikardt C, Sapru HN, and Kuzhikandathil EV (2014) Overexpression of the dopamine D3 receptor in the rat dorsal striatum induces dyskinetic behaviors. *Behav Brain Res* **263**:46–50.
- de Bartolomeis A, Buonaguro EF, Latte G, Rossi R, Marmo F, Iasevoli F, and Tomasetti C (2017) Immediate-early genes modulation by antipsychotics: translational implications for a putative gateway to drug-induced long-term brain changes. *Front Behav Neurosci* **11**:240.
- Feyder M, Bonito-Oliva A, and Fisone G (2011) L-DOPA-induced dyskinesia and abnormal signaling in striatal medium spiny neurons: focus on dopamine D1 receptor-mediated transmission. *Front Behav Neurosci* **5**:71.
- Fleischhacker W, Galderisi S, Laszlovsky I, Szatmári B, Barabássy Á, Acsai K, Szalai E, Harsányi J, Earley W, Patel M, et al. (2019) The efficacy of cariprazine in negative symptoms of schizophrenia: post hoc analyses of PANSS individual items and PANSS-derived factors. *Eur Psychiatry* **58**:1–9.
- Fumagalli F, Frasca A, Racagni G, and Riva MA (2009) Antipsychotic drugs modulate Arc expression in the rat brain. *Eur Neuropsychopharmacol* **19**:109–115.
- Garnock-Jones KP (2017) Cariprazine: a review in schizophrenia. *CNS Drugs* **31**: 513–525.
- Goddard WA III and Abrol R (2007) 3-Dimensional structures of G protein-coupled receptors and binding sites of agonists and antagonists. *J Nutr* **137** (6 Suppl 1): 1528S–1538S, discussion 1548S.
- Iderberg H, Francardo V, and Pioli EY (2012) Animal models of L-DOPA-induced dyskinesia: an update on the current options. *Neuroscience* **211**:13–27.
- Jerlhag E, Janson AC, Waters S, and Engel JA (2012) Concomitant release of ventral tegmental acetylcholine and accumbal dopamine by ghrelin in rats. *PLoS One* **7**: e49557.
- Kalia LV and Lang AE (2015) Parkinson's disease. *Lancet* **386**:896–912.
- Kiss B, Horváth A, Némethy Z, Schmidt E, Laszlovsky I, Bugovics G, Fazekas K, Hornok K, Orosz S, Gyertyán I, et al. (2010) Cariprazine (RGH-188), a dopamine D(3) receptor-preferring, D(3)/D(2) dopamine receptor antagonist-partial agonist antipsychotic candidate: in vitro and neurochemical profile. *J Pharmacol Exp Ther* **333**:328–340.
- Krack P, Martinez-Fernandez R, Del Alamo M, and Obeso JA (2017) Current applications and limitations of surgical treatments for movement disorders. *Mov Disord* **32**:36–52.
- Lacroix LP, Ceolin L, Zocchi A, Varnier G, Garzotti M, Curcuruto O, and Heidbreder CA (2006) Selective dopamine D3 receptor antagonists enhance cortical acetylcholine levels measured with high-performance liquid chromatography/tandem mass spectrometry without anti-cholinesterases. *J Neurosci Methods* **157**:25–31.
- Li P, Snyder GL, and Vanover KE (2016) Dopamine targeting drugs for the treatment of schizophrenia: past, present and future. *Curr Top Med Chem* **16**:3385–3403.
- Lundblad M, Usiello A, Carta M, Håkansson K, Fisone G, and Cenci MA (2005) Pharmacological validation of a mouse model of l-DOPA-induced dyskinesia. *Exp Neurol* **194**:66–75.
- Magnusson O, Fowler CJ, Köhler C, and Ogren SO (1986) Dopamine D2 receptors and dopamine metabolism. Relationship between biochemical and behavioural effects of substituted benzamide drugs. *Neuropharmacology* **25**:187–197.
- Malo M, Brive L, Luthman K, and Svensson P (2010) Selective pharmacophore models of dopamine D(1) and D(2) full agonists based on extended pharmacophore features. *ChemMedChem* **5**:232–246.
- Malo M, Brive L, Luthman K, and Svensson P (2012) Investigation of D2 receptor-agonist interactions using a combination of pharmacophore and receptor homology modeling. *ChemMedChem* **7**:471–482, 338.
- Marcellino D, Ferré S, Casadó V, Cortés A, Le Foll B, Mazzola C, Drago F, Saur O, Stark H, Soriano A, et al. (2008) Identification of dopamine D1-D3 receptor heteromers. Indications for a role of synergistic D1-D3 receptor interactions in the striatum. *J Biol Chem* **283**:26016–26025.
- Marcus MM, Wiker C, Frånberg O, Konradsson-Geuken A, Langlois X, Jardemark K, and Svensson TH (2010) Adjunctive alpha2-adrenoceptor blockade enhances the antipsychotic-like effect of risperidone and facilitates cortical dopaminergic and glutamatergic, NMDA receptor-mediated transmission. *Int J Neuropsychopharmacol* **13**:891–903.
- Mewshaw RE, Kavanagh J, Stack G, Marquis KL, Shi X, Kagan MZ, Webb MB, Katz AH, Park A, Kang YH, et al. (1997) New generation dopaminergic agents. 1. Discovery of a novel scaffold which embraces the D2 agonist pharmacophore. Structure-activity relationships of a series of 2-(aminomethyl)chromans. *J Med Chem* **40**:4235–4256.
- Muir KW and Lees KR (1995) Clinical experience with excitatory amino acid antagonist drugs. *Stroke* **26**:503–513.
- Németh G, Laszlovsky I, Czobor P, Szalai E, Szatmári B, Harsányi J, Barabássy Á, Debelle M, Durgam S, Bitter I, et al. (2017) Cariprazine versus risperidone monotherapy for treatment of predominant negative symptoms in patients with schizophrenia: a randomised, double-blind, controlled trial. *Lancet* **389**:1103–1113.
- Paxinos G and Watson C (1986) *The Rat Brain in Stereotaxic Coordinates*, Academic Press, Sydney.
- Payer DE, Guttman M, Kish SJ, Tong J, Adams JR, Rusjan P, Houle S, Furukawa Y, Wilson AA, and Boileau I (2016) D3 dopamine receptor-preferring [11C]PHNO PET imaging in Parkinson patients with dyskinesia. *Neurology* **86**:224–230.
- Ponten H, Kullingsjö J, Lagerkvist S, Martin P, Pettersson F, Sonesson C, Waters S, and Waters N (2010) In vivo pharmacology of the dopaminergic stabilizer prido-pidine. *Eur J Pharmacol* **644**:88–95.
- Rascol O, Perez-Lloret S, and Ferreira JJ (2015) New treatments for levodopa-induced motor complications. *Mov Disord* **30**:1451–1460.
- Robbins MJ, Critchlow HM, Lloyd A, Cilia J, Clarke JD, Bond B, Jones DN, and Maycox PR (2008) Differential expression of IEG mRNA in rat brain following acute treatment with clozapine or haloperidol: a semi-quantitative RT-PCR study. *J Psychopharmacol* **22**:536–542.
- Sharma VD, Lyons KE, and Pahwa R (2018) Amantadine extended-release capsules for levodopa-induced dyskinesia in patients with Parkinson's disease. *Ther Clin Risk Manag* **14**:665–673.
- Solis O, Garcia-Montes JR, González-Granillo A, Xu M, and Moratalla R (2017) Dopamine D3 receptor modulates l-DOPA-induced dyskinesia by targeting D1 receptor-mediated striatal signaling. *Cereb Cortex* **27**:435–446.
- Solis O and Moratalla R (2018) Dopamine receptors: homomeric and heteromeric complexes in L-DOPA-induced dyskinesia. *J Neural Transm (Vienna)* **125**: 1187–1194.
- Sonesson C, Karlsson J, and Svensson P (2012) inventors. Novel modulators of cortical dopaminergic- and nmda-receptor-mediated glutamatergic neurotransmission, IRLAB. WO2012143337. Publication Date 2012-10-26
- Stahl SM (2017) Drugs for psychosis and mood: unique actions at D3, D2, and D1 dopamine receptor subtypes. *CNS Spectr* **22**:375–384.
- Svenningsson P, Johansson A, Nyholm D, Tsitsi P, Hansson F, Sonesson C, and Tedroff J (2018) Safety and tolerability of IRL790 in Parkinson's disease with levodopa-induced dyskinesia-a phase 1b trial. *NPJ Parkinsons Dis* **4**:35.
- Teber I, Köhling R, Speckmann EJ, Barnekow A, and Kremerskothen J (2004) Muscarinic acetylcholine receptor stimulation induces expression of the activity-regulated cytoskeleton-associated gene (ARC). *Brain Res Mol Brain Res* **121**: 131–136.
- Tresadern G, Bartolome JM, Macdonald GJ, and Langlois X (2011) Molecular properties affecting fast dissociation from the D2 receptor. *Bioorg Med Chem* **19**: 2231–2241.
- Vermeiren Y and De Deyn PP (2017) Targeting the norepinephrine system in Parkinson's disease and related disorders: the locus coeruleus story. *Neurochem Int* **102**:22–32.
- Villalba RM and Smith Y (2018) Loss and remodeling of striatal dendritic spines in Parkinson's disease: from homeostasis to maladaptive plasticity? *J Neural Transm (Vienna)* **125**:431–447.
- Wang S, Che T, Levit A, Shoichet BK, Wacker D, and Roth BL (2018a) Structure of the D2 dopamine receptor bound to the atypical antipsychotic drug risperidone. *Nature* **555**:269–273.
- Wang WW, Zhang XR, Zhang ZR, Wang XS, Chen J, Chen SY, and Xie CL (2018b) Effects of mGluR5 antagonists on Parkinson's patients with L-dopa-induced dyskinesia: a systematic review and meta-analysis of randomized controlled trials. *Front Aging Neurosci* **10**:262.
- Waters N, Lagerkvist S, Löfberg L, Piercey M, and Carlsson A (1993) The dopamine D3 receptor and autoreceptor preferring antagonists (+)-A-J76 and (+)-UH232; a microdialysis study. *Eur J Pharmacol* **242**:151–163.
- Waters S, Ponten H, Edling M, Svanberg B, Klammer D, and Waters N (2014) The dopaminergic stabilizers prido-pidine and ordopidine enhance cortico-striatal Arc gene expression. *J Neural Transm (Vienna)* **121**:1337–1347.
- Waters S, Svensson P, Kullingsjö J, Pontén H, Andreasson T, Sunesson Y, Ljung E, Sonesson C, and Waters N (2017) In vivo systems response profiling and multi-variate classification of CNS active compounds: a structured tool for CNS drug discovery. *ACS Chem Neurosci* **8**:785–797.
- Wesołowska A and Kowalska M (2008) Influence of serotonin 5-HT(7) receptor blockade on the behavioral and neurochemical effects of imipramine in rats. *Pharmacol Rep* **60**:464–474.

**Address correspondence to:** Susanna Waters, Integrative Research Laboratories Sweden AB, A Wallgrens Backe 20, SE 41346 Göteborg, Sweden. E-mail: susanna.waters@irlab.se